ELSEVIER

Polymer 44 (2003) 1819–1834

polymer

www.elsevier.com/locate/polymer

Relation of glass transition temperature to the hydrogen bonding degree and energy in poly(*N*-vinyl pyrrolidone) blends with hydroxyl-containing plasticizers: 3. Analysis of two glass transition temperatures featured for PVP solutions in liquid poly(ethylene glycol)

Mikhail M. Feldstein[a,*], Alexandra Roos[b], Cédrick Chevallier[b], Costantino Creton[b], Elena E. Dormidontova[c,1]

[a]*A.V. Topchiev Institute for Petrochemical Synthesis, Russian Academy of Sciences, 29 Leninsky prospekt, 119991 Moscow, Russia*

[b]*Laboratoire de Physico-Chimie Structurale et Macromoléculaire, Ecole Supérieure de Physique et de Chimie Industrielles de la ville de Paris (ESPCI), 10, rue Vauquelin, 75231 Paris Cedex 05, France*

[c]*Department of Chemical Engineering and Materials Science, University of Minnesota, 421 Washington Ave. SE, Minneapolis, MN 55455, USA*

Received 31 July 2002; received in revised form 5 December 2002; accepted 13 January 2003

Abstract

The phase behaviour of poly(*N*-vinyl pyrrolidone)–poly(ethylene glycol) (PVP–PEG) blends has been examined in the entire composition range using Temperature Modulated Differential Scanning Calorimetry (TM-DSC) and conventional DSC techniques. Despite the unlimited solubility of PVP in oligomers of ethylene glycol, the PVP–PEG system under consideration demonstrates two distinct and mutually consistent glass transition temperatures (T_g) within a certain concentration region. The dissolution of PVP in oligomeric PEG has been shown earlier (by FTIR spectroscopy) to be due to hydrogen bonding between carbonyl groups in PVP repeat units and complementary hydroxyl end-groups of PEG chains. Forming two H-bonds through both terminal OH-groups, PEG acts as a reversible crosslinker of PVP macromolecules. To characterise the hydrogen bonded complex formation between PVP ($M_w = 10^6$) and PEG ($M_w = 400$) we employed an approach described in the first two papers of this series that is based on the modified Fox equation. We evaluated the fraction of crosslinked PVP units and PEG chains participating to the complex formation, the H-bonded network density, the equilibrium constant of complex formation, etc. Based on the established molecular details of self-organisation in PVP–PEG solutions, we propose a three-stage mechanism of PVP–PEG H-bonded complex formation/breakdown with increase of PEG content. The two observed T_gs are assigned to a coexisting PVP–PEG network (formed via multiple hydrogen bonding between a PEG and PVP) and a homogeneous PVP–PEG blend (involving a single hydrogen bond formation only). Based on the strong influence of coexisting regions on each other and the absence of signs of phase separation (evidenced by Optical Wedge Microinterferometry) we conclude that the PVP–PEG blend is fully miscible on a molecular scale.

Keywords: Poly(*N*-vinyl pyrrolidone) blends with poly(ethylene glycol); Glass transition temperature; Effect of hydrogen bonding

1. Introduction

Miscibility in polymer–polymer mixtures has been the subject of considerable interest, discussions and debates in the literature [1,2]. Miscibility at the molecular scale is not necessarily homogeneous within the entire range of composition and temperatures: interactions between similar or different macromolecules may lead to a certain amount of clustering or other non-uniform arrangement of polymer segments. The questions about miscibility are almost never raised in those comparatively rare cases where one polymer is known to be completely soluble in a different polymer, such that the two may be regarded as solute and solvent [1].

In many blends, a homogeneous phase is obtained because of the existence of specific favourable interactions between different polymer components, which allow mixing on a molecular scale. One such favourable interaction is

* Corresponding author. Fax: +7-095-230-22-24.
E-mail address: mfeld@ips.ac.ru (M.M. Feldstein).
[1] Present address: Department of Macromolecular Science and Engineering, Case Western Reserve University, 337 Kent Hale Smith Building, 2100 Adelbert Road, Cleveland, OH 44106, USA.

0032-3861/03/$ - see front matter © 2003 Elsevier Science Ltd. All rights reserved.
doi:10.1016/S0032-3861(03)00046-6

hydrogen bonding that has been reported for many polymer blends [3–11]. Polymers containing ternary amide groups, such as poly(*N*-vinyl pyrrolidone) (PVP), are potentially good proton acceptors due to the basic nature of the functional groups [12] At the same time, short-chain poly(ethylene glycol) (PEG) carries two proton-donating hydroxyl groups at the chain ends [13–15]. Unlimited PVP solubility in liquid PEG is well established [16,17], and the PVP–PEG blends may be therefore treated as the solutions of high molecular weight PVP in liquid oligo(ethylene glycols).

It has been determined by FTIR spectroscopy that PVP–PEG miscibility is due to hydrogen-bonding between the hydrogen atom of PEG terminal groups and electronegative oxygen atom in the carbonyl groups of the monomer units of the PVP chains [18,19]. High molecular weight PVP is only soluble in short-chain PEGs [20,21], ranging in molecular weight from 200 to 600 g/mol. As is shown by direct Optical Wedge Microinterferometry (WMI) measurement of PVP–PEG spontaneous mixing [17,22], no phase boundary occurs between glassy PVP and liquid PEG-400, indicating unequivocally that the PVP–PEG blend is a single-phase, miscible system.

The most unambiguous experimental evidence of polymer miscibility is the occurrence of a single glass transition temperature, which is intermediate between the two T_gs corresponding to the blend components [1]. In miscible blends, the glass transition temperature generally depends on blend composition through a simple rule of mixing, outlined by the Fox equation [23]. At the other extreme, blends of immiscible polymers that segregate into distinct phases exhibit glass transitions identical in their temperature to that of the unblended components. In the intermediate cases of partial polymer miscibility or if the size of the dispersed phase is very small, the T_gs of individual components may be shifted, hindering the distinction between miscible blends and the systems of where only partial miscibility is present. An elevation in temperature of the low-T_g transition and a depression of the high-T_g transition in a two-phase polymer blends may indicate that the system is very close to being miscible. On the other hand, the coincidence of the component T_gs with those of the unblended polymers is indicative of phase separation [24].

As has been shown in recent studies on the phase behaviour of PVP-solutions in PEG, the essential feature of polymer blends exhibiting miscibility on a molecular scale is the coherence of thermal transitions [25–27]. By "coherence" we mean here the feature of thermal transitions in miscible blend when all the transition temperatures and relevant amplitudes maintain a specific, logically connected and integrated relationship to each other and to the blend composition. Indeed, for the polymer blends which miscibility is achieved by specific favourable interactions between the components, the change in concentration of any component affects simultaneously the phase behaviour of entire system. The PVP is an amorphous polymer, while PEG is capable of forming a crystalline phase, and the third component of a PVP–PEG blend is a low molecular weight volatile liquid (water, sorbed from the surrounding atmosphere or residual after blend preparation). The DSC technique enables the characterisation of the states of every blend components and their interactions by observing the compositional behaviour of the amorphous and crystalline phases coupled with the examination of the vaporisation endotherms of the liquid component [27]. Upon heating, a heat capacity jump followed by single exotherm (coupled with a symmetric endotherm, and a high temperature endotherm) is normally observed for PVP–PEG blends. These four transitions were attributed, respectively, to: the glass transition, PEG cold crystallisation, melting, and water thermodesorption [25]. The coherence in the compositional behaviour of all these four transitions was established by heating the PVP–PEG blends of various hydration [25–27].

The glass transition temperature, T_g, is one of the most fundamental features of polymers. The T_g relates directly to the cohesive energy and packing density [28,29]. The simple rule of mixing, stated by the Fox equation [23], neglects specific interactions between polymer and plasticizer, inferring a complete uniformity of intermolecular forces. In practice, the plasticization effect involves often the specific interactions or excess volume formation upon mixing the polymer and plasticizer (solvent), which lead to the negative T_g deviations. Large negative T_g deviations (from the Fox equation) have been recently observed for PVP blends with plasticizers bearing two and more hydroxyl groups (PEG and glycerol) [20,21]. The difference between measured T_g values and those predicted with the Fox equation is usually considered as a measure of the strength of interactions between molecules of blended components. Numerous equations have been proposed over past years to describe the effects of interaction, excess volume formation and chain orientation on the composition dependence of T_g. In order to gain an insight into the PVP–PEG interaction mechanism, the analysis of compositional T_g behaviour of this blend has been recently performed [30] applying the equations proposed by Gordon and Taylor [31], Couchman and Karasz [32], Kovacs, Braun and Kovacs [33], Kwei [34], Breckner et al. [35]. Unfortunately, these equations did not provide an estimate of the number of hydrogen bonds formed in the PVP–PEG blends.

A simple method of evaluation of the binding degree and energy from the T_g–composition relationships has been suggested in the first two papers of this series where it was applied to the blends of PVP with PEG and other hydroxyl-containing plasticizers: ethanol, water and glycerol [20,21]. This approach represents a modification of the Fox equation, which has been found to describe reasonably well the T_g behaviour of the polymer blends with specific interactions when the weight fractions of components are replaced by the mole fractions of the corresponding reactive functional groups [36].

To fit the T_g for PVP–PEG hydrated blends, an adjusting parameter, w^*_{PEG}, was introduced into the original form of the Fox equation [20,21]:

$$\frac{1}{T_g} = \frac{w_{PVP}}{T_{g_{PVP}}} + \frac{w_{H_2O}}{T_{g_{H_2O}}} + \frac{w_{PEG} + w^*_{PEG}}{T_{g_{PEG}}} \quad (1)$$

where T_g refers to the glass transition temperatures and w to the weight fractions of PVP, water and PEG, respectively.

Within the context of Eq. (1) the parameter w^*_{PEG} has a clear physical meaning. Since the negative deviations are established to result only from the formation of more than one hydrogen bond (e.g. through both terminal OH groups in PEG molecule), w^*_{PEG} defines the weight fraction of PEG chains crosslinking the repeat units in PVP chains by means of two H-bonds. According to Eq. (1), the $(w_{PEG} + w^*_{PEG})/w_{PEG}$ quantity is the number of hydroxyl groups per plasticizer molecule, involved into H-bonding with PVP. Indeed, as is obviously demonstrated in the first paper of this series [20], with the decrease in plasticizer concentration in blends, this quantity tends to unity for water and ethanol, two for PEG and three for glycerol that contains three reactive OH groups per molecule. Through the w^*_{PEG} parameter the following quantities may be easily predicted: the fractions of PEG hydroxyl groups (and PEG chains) crosslinking the PVP units by 2 H-bonds, the fraction of PVP repeat units crosslinked by H-bonding through PEG chains, the equilibrium constant and free energy of the PVP–PEG network complex formation [20,21]. In the context of this paper the word 'complex' refers to the product of PVP–PEG interaction when a PEG chain forms simultaneously two H-bonds with PVP monomer units through both terminal hydroxyls. Being in a thermodynamic equilibrium each H-bond forms and breaks with a characteristic time. Capability of hydrogen bonds formation in the system can be characterised by the average number of PEG chains with two H-bonds, which is a function of blend composition and temperature.

The dissolution of PVP in short-chain PEG has been shown to be a two-stage process [30]. The first stage may be defined as a plasticization of the PVP, whereas the second stage consists of a gradual dissolution of the plasticized PVP in an excess of PEG. The blend containing 36 wt% PEG was identified as a boundary between two stages [30].

While the molecular mechanism underlying the second stage of the spontaneous mixing process of PVP and PEG is clearly observed by DSC [18,19,21,25–27,30] and confirmed with WMI [17,22] and Pulsed Field Gradient (PFG) NMR [37,38] techniques, the details of the most important mechanism of formation of the PVP–PEG H-bond complex in the blends containing less than 36% of PEG are hidden by the occurrence of two glass transition temperatures [19]. The lower T_g has been unequivocally established to be related to the PVP–PEG hydrogen bonded network [18,19,21,25–27,30], whereas the upper T_g was supposed to outline the composition behaviour of a non-equilibrium phase composed by PVP plasticized with small amounts of PEG and water [19]. Therefore, the product of PVP–PEG interaction was considered to be immiscible with the parent PVP in the blends containing less PEG than what was required to form fully the network complex. Previous attempts to explore this issue in more detail with conventional DSC have failed due to the overlap of the upper glass transition with the endotherm of water vaporisation.

The Temperature Modulated Differential Scanning Calorimetry (TM-DSC) is a relatively new technique [39–43], where a polymer sample is subjected to a linear heating ramp with a superimposed low frequency sinusoidal temperature oscillation (modulation) resulting in a modulation of the heating profile. Deconvolution of the calorimetric response (Fourier transform method) enables the separation of reversible and irreversible (within the modulation time scale) thermal phenomena occurring during the thermal treatment. The reversing signal is excellent for quantifying the glass transition with a great precision, and separates the glass transition completely from other non-reversing processes such as cold crystallisation and vaporisation, which have been shown to occur in PVP–PEG hydrogels [25–27]. In this work, the TM-DSC technique is employed to shed light upon the mechanism of PVP–PEG complexation within those PVP blends containing less than 50% of PEG, and the data are compared with those described earlier for the blends ranging in PEG content from 36 to 100% [18,19,21,25–27,30]. With the help of this new method, the behaviour of both T_gs has been now analysed within the entire PVP–PEG composition range.

This paper is intended to serve two purposes. First, it continues the series of two earlier papers [20,21] and demonstrates how the approach described in the first two papers of the series (that allows evaluating of the degree of hydrogen bonding and the energy of PVP–PEG network complex formation) can also be applied to the complex systems featuring two T_gs. Second, this paper is also aimed to improve our insight into the mechanism of PVP–PEG interaction based on DSC data. This paper is a part of a general effort to understand the behaviour of PVP–PEG blends. Considerable progress has been already achieved in studying the molecular mechanism of PVP–PEG interaction (by FTIR Spectroscopy [18,19,21]), the phase state of PVP–PEG blends (by DSC and WAXS [18–21,25–27,30]), kinetics of PVP dissolution in PEG (by WMI [17,22]), the viscoelastic properties of H-bonded network in PVP–PEG blends (by rheological measurements [18,38,39,44]), coupled with the physical properties of PVP–PEG composites over the entire composition range, such as molecular mobility (by PFG NMR [17,22]) and pressure-sensitive adhesion [45–52].

2. Experimental

PVP (Kollidon K-90), $M_w = 1,000,000$ g/mol, and PEG (Lutrol E-400), $M_w = 400$ g/mol, were obtained from BASF. The polymers were used as received.

The PVP blends with PEG, covering a full range of compositions, were prepared by dissolving both polymers in a common solvent (ethyl alcohol). The solutions were poured in teflon moulds (2 cm-deep) and remained at room temperature during 7 days in order to evaporate most of the solvent. The resulting films (1–1.5 mm-thick) were then dried 3 h under vacuum, at 65 °C. Removal of ethyl alcohol from prepared blends was ascertained by FTIR spectroscopy by the absence of methylene group stretching vibrations at 2974 and 1378 cm^{-1} using a Bruker IFS-113v spectrometer with a resolution of 1 cm^{-1} after averaging from 128 scans. The freshly prepared blends and unblended PVP were then stored for 6 days at ambient temperature by equilibrating them at a controlled pressure of water vapor in a dessiccator containing an aqueous H_2SO_4 solution of $d = 1.29$ g/cm^3, maintaining RH = 53% at 25 °C. Under these conditions the water content of the blends averaged 12 wt%.

In the TM-DSC or DSC apparatus the samples were first quench cooled with liquid nitrogen from ambient temperature to −150 °C at a cooling rate of 10 °C min^{-1}, subjected to isothermal annealing at this temperature and then heated up to 220 °C at a rate of 5 °C min^{-1}. For the TM-DSC measurements, the constant heating rate was superimposed with a temperature modulation with a period of 60 s and amplitude of ±0.796 °C. The respective T_gs were recorded at inflection points of the relevant heat capacity jumps using a TA Instruments Universal Analysis 2000 software supplied with microcalorimeter. The TM-DSC heating thermograms were measured with a 2820 Modulated Differential Scanning Calorimeter (TA Instruments), whereas the DSC heating traces were obtained with a Mettler TA 4000/DSC 30 thermoanalyzer, calibrated with indium and gallium. Heats of the PEG melting peaks were computed by constructing linear baselines from the peak onset to completion and numerically integrated with appropriate software supplied by Mettler. All reported values are the average of replicate experiments varying less than 1–2%. In order to avoid the superposition of the glass transition response with other thermal events, in the TM-DSC tests the heating scans were analysed by the TA Universal Analysis software using the reversible heat flux only. All the TM-DSC measurements were performed with the samples hermetically sealed in aluminum pans in order to avoid water evaporation. It was important to ensure a perfect contact between the pans and the heating cell and to have very flat pans. In contrast, in the conventional DSC measurements the samples of 5–15 mg in weight were sealed in standard aluminum pans supplied with pierced lids so that absorbed moisture could evaporate upon heating. An argon purge (50 ml min^{-1}) was used to avoid moisture condensation at the sensor.

The weight fractions of crystalline PEG in the blends with amorphous PVP, w_{crPEG}, have been calculated as the ratios of appropriate heats of melting, ΔH_m, of blended PEG to the reference values for unblended PEG, taking into account the weight fraction of absorbed water, w_{H_2O} :

$$w_{crPEG} = \frac{\Delta H_m(\text{blend})}{\Delta H_{mPEG}(1 - w_{H_2O})} \quad (2)$$

The ΔH_m reference value of unblended crystalline PEG-400 was 122.1 J/g [25].

The content of absorbed water in the blends was determined gravimetrically by the termination of weight loss upon drying in vacuum. In addition, the content of water was also measured by weighing the samples before and after DSC scans using a Mettler Analytical Balance, AE 240, with an accuracy of ±0.01 mg. Weight loss of the sample after scanning was compared to the amount of desorbed water evaluated from the enthalpy change associated with water evaporation from the sample by DSC [27].

3. Results and discussion

3.1. General description of the phase behaviour of PVP-rich blends

TM-DSC heating thermograms for PVP and PVP–PEG blends of 12% hydration are shown in Figs. 1 and 2 for compositions ranging between 0 and 50% PEG. The scan of unblended PVP reveals a broad symmetric endotherm of water vaporisation at 90 °C, followed by a heat capacity jump at the glass transition ($T_g = 179.2$ °C, $\Delta C_p = 0.122$ J/g K). No freezing water is detected in hydrated PVP even if the content of water is as large as 20%. The data match closely those obtained earlier with conventional DSC [25]. The DSC heating curve of dry PEG-400 is reported to display the glass transition at $T_g = -70$ °C, $\Delta C_p = 0.32$ J/g K and fusion endotherm at $T_m = 6$ °C, $\Delta H_m = 118.4$ J/g [25]. Since the PVP and PEG T_gs differ by a value of about 250 °C, the peculiarities of the composition dependence of T_g in these blends are easily discernible with the TM-DSC technique that separates the glass transition jump from the background of the overlapping vaporisation endotherm (Fig. 1).

Adding PEG-400 to the glassy PVP results first in a smooth decrease of the observed single glass transition to lower values. This is observed up to 10 wt% PEG as shown in Figs. 1 and 3. As the PEG content increases to 20%, a second glass transition appears in a lower temperature region. Two different T_gs are mostly pronounced for the PVP blends with 31 and 35% PEG (Fig. 2), although the TA Instruments Universal Analysis 2000 software has also detected two inflection points for other blends containing 20 and 41% PEG. Two factors have effect on the appearance of

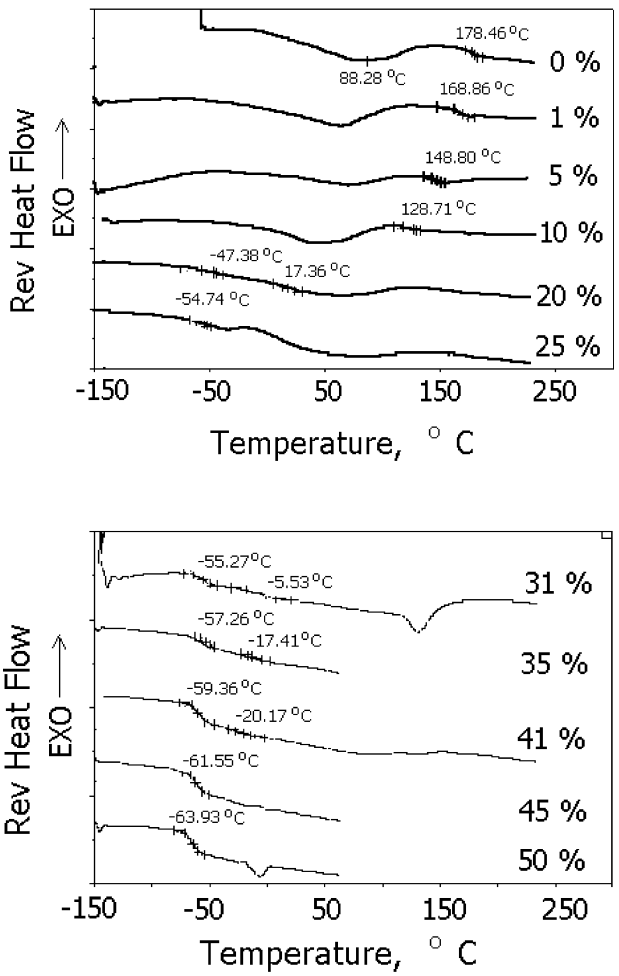

Fig. 1. TM-DSC traces of heating of PVP–PEG blends containing different amounts of PEG-400 and in average 12% of sorbed water.

two T_gs. First, the fraction of specific T_g-phase in blend should be appreciable. This is not the case for the blends containing less than 20% PEG. Second, values of the two T_g should differ at least by 40 °C (Fig. 2). This requirement is not satisfied for the blends containing more than 41% PEG. Although both T_gs are composition dependent, decreasing with increasing PEG concentration, the plasticizing effect of PEG-400 is mainly affecting the upper T_g that drops more rapidly upon subsequent addition of PEG (Fig. 3). As the PEG concentration in the blends reaches 45%, the upper glass transition vanishes. A physicochemical identification of the upper and lower-T_g phases requires the analysis of the composition dependence of the T_gs within the entire composition range and is considered in the following sections of this paper.

If no appreciable interaction between polymer components in a blend occurs, the change in heat capacity at the glass transition (ΔC_p) can be taken as a measure of the relative amount of the phase with a specified T_g value. As Tanaka has shown [53], the ΔC_p is a sum of three contributions: conformational, free volume and cohesive interactions. While the conformational contribution is relatively negligible, the smaller the free volume and the greater the energy of cohesive interactions, the higher the ΔC_p. Since the PVP–PEG miscible blends are formed through hydrogen bonding that affects appreciably the composition dependence of both free volume and cohesive interaction energy, the change in heat capacity associated with the upper and lower T_g-transitions can not be regarded as a characteristic of the relative amount of each phase. As follows from the data displayed in Fig. 4, the ΔC_p of the upper T_g-phase reveals no explicit relation to the blend composition and in a first approximation can be considered as a constant value, $\Delta C_p = 0.14 \pm 0.02$ J/g K ($p = 2.75 \times 10^{-5}$). In contrast, the ΔC_p of the lower T_g-phase exhibits a cooperative S-shaped transition, increasing rapidly with the rise in PEG content within a very narrow composition range between 35 and 40% of PEG-400. This ΔC_p elevation cannot be explained by the disappearance of the upper T_g-phase that occurs at somewhat larger PEG content (Fig. 3). As is shown in Fig. 5, the ΔC_p transition at 35% PEG concentration is immediately followed by the crystallisation of PEG (at PEG content 50% and higher). The crystallising PEG can be considered as that uninvolved into amorphous PVP–PEG complex [23,26], and a sharp elevation in ΔC_p outlines therefore the boundary between the stages of PVP–PEG crosslinked H-bond complex formation and mixing of the complex with PEG excess.

Thus, the phase behaviour of the PVP–PEG blends within the two T_g composition region is typical of a two-phase system. However, as has been earlier unambiguously established by direct observation of PEG spontaneous mixing with PVP using the WMI technique [17,22], this system is completely miscible. With the WMI technique both mutual diffusion of blend components and phase separation can be easily visualised and characterised quantitatively. The same conclusion has been also inferred from the consistency in the behaviour of all four thermal transitions occurring in PVP–PEG blends above 35% PEG concentration [25–27]. Consequently, in order to describe firmly the PVP–PEG system as truly miscible or close to be miscible on a molecular scale within the PVP-rich composition range, the coherence among the two measured glass transitions has to be analysed.

3.2. The upper glass transition temperature

Fig. 3 plots both T_gs evaluated by the TM-DSC technique against the composition of PVP–PEG blends. The lower T_g has been established earlier to characterise the PVP–PEG H-bond network complex [21]. This T_g is easily detectable by a conventional DSC technique. Its compositional behaviour [22], relationship to other thermal transitions [25–27] and to the stoichiometry of PVP–PEG H-bonding [18–21] have been recently analysed in full details for the PVP blends containing 35 wt% of PEG-400 and more. Agreement is excellent among T_gs evaluated using TM-DSC and DSC methods for the blends of identical

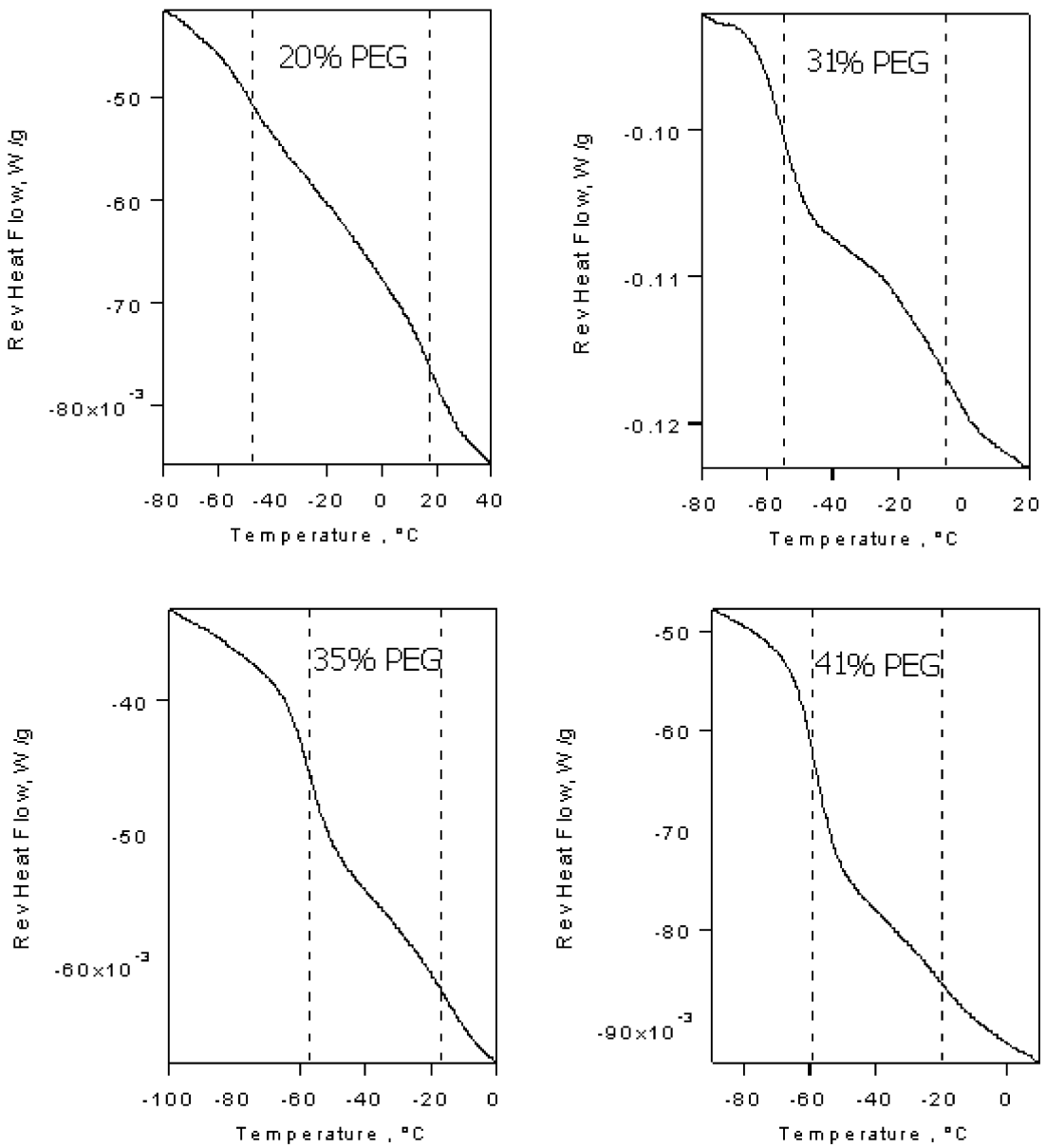

Fig. 2. The heat capacity jumps relating to the blends exhibiting two glass transitions. The dashed line is positioned at the temperature where the software has detected the inflection point.

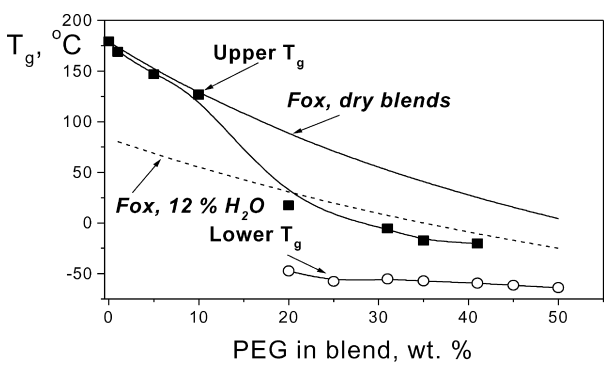

Fig. 3. Relation of glass transition temperatures to the composition of PVP blends containing 0–50 wt% PEG.

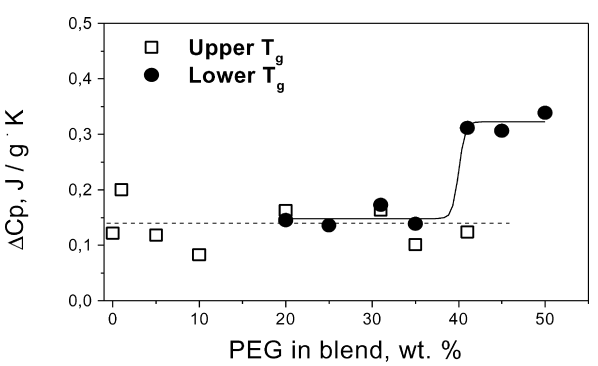

Fig. 4. The change in heat capacity at glass transition (ΔC_p) as a function of PVP–PEG blend composition.

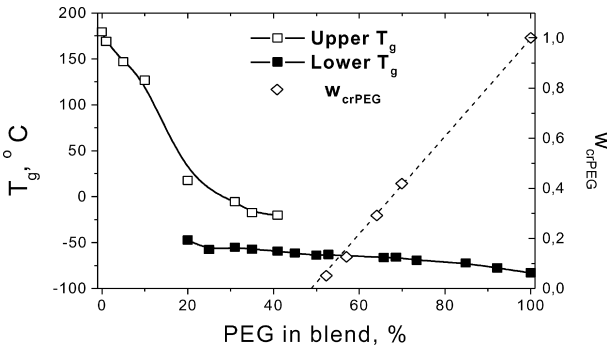

Fig. 5. Compositional dependence of the glass transition temperature and the weight fraction of crystalline PEG in the blends with amorphous PVP.

composition and hydration, tested under the same heating rate. Thus, the PVP blend with 35 wt% of PEG-400 revealed a $T_g = -57.26$ °C by TM-DSC and -57.3 °C by conventional DSC [25]. Combining the TM-DSC and DSC data, we can now describe the phase behaviour of the PVP–PEG system over the entire composition range (Fig. 5).

As is evident from the data in Fig. 3, an unambiguous attribution of the upper T_g-phase is straightforward when the composition dependence of the upper T_g satisfies a simple weight-average rule of mixing, such as the Fox equation (1) at $w^*_{PEG} = 0$ [23]. At low PEG content in blends (0–10%), the T_g is preceded by a water vaporisation endotherm (Fig. 1) and the composition dependence of the upper T_g follows the pattern predicted by the Fox rule of mixing for dry PVP–PEG blends. Under a subsequent increase in PEG concentration (20–40%), the upper T_g drops below the temperature of water evaporation (Fig. 1) and obeys to some extent the Fox rule for the blends of 12% hydration, demonstrating comparatively small negative deviations from predicted values. The implication of these deviations is discussed below, in the Section 3.7 of this paper. The success of the Fox equation in describing the composition dependence of the upper T_g-phase unequivocally implies the miscibility of PVP with PEG-400. But there is still the question of whether this mixing occurs on a molecular scale. In other words, is the PVP miscible with PEG, or is the blend very close to being miscible? To answer this question, a molecular insight into the PVP–PEG interaction mechanism is needed, and such insight can be provided by the analysis of the composition dependence of the lower T_g. Such analysis can be performed using a simple algorithm proposed recently in two preceding papers of this series [20,21].

3.3. The lower T_g analysis

As is seen from Fig. 5, the value of the lower T_g in PVP–PEG blends matches closely that found for unblended PEG-400 at a comparable degree of hydration. Nevertheless, the lower T_g cannot be attributed to the occurrence of unblended PEG phase within the blends containing 20–40% of PEG due to following reasons:

1. If the lower T_g belonged to the unblended PEG phase, the composition dependence of the upper T_g would display positive deviations from the values predicted by the Fox equation.
2. PEG-400 is a crystalline polymer, however its blends with amorphous PVP develop no crystallinity at PEG contents lower than 45 wt% (Fig. 1) [18,19,21,25–27]. The weight fraction of crystallising PEG in the blends, evaluated from the composition dependence of the heat of PEG fusion using Eq. (2), is plotted in Fig. 5 along with both T_gs vs. PEG content. If there is a macrophase separation into PVP-rich and PEG-rich phases, the latter would be crystallized and the plot would represent a straight line connecting the origin and the point of $w_{crPEG} = 1$. However, this is evidently not what is happening according to Fig. 5. Apparently PEG is strongly involved into formation of specific interactions (hydrogen bonding) with PVP and does not form a separate crystalline phase. The intercept of the w_{crPEG} plot versus PEG concentration in Fig. 5 at $w_{crPEG} = 0$ represents the amount of non-crystallising (H-bonded) PEG in the blends [21,26]. The degree of PEG binding, evaluated by DSC and WAXS techniques (from the composition behaviour of blend crystallinity) agrees well with that found with independent methods (FTIR spectroscopy, T_g analysis) [19,21].

Thus, the lower T_g relates unambiguously to some amorphous PVP–PEG interaction product that has nucleated and grows within the upper T_g-phase, which represents a homogeneous PVP–PEG mixture.

3.4. Cooperative character of the PVP–PEG interaction

Large negative T_g deviations from the relationship predicted by the Fox equation are the evidence of strong specific PVP–PEG interactions. To gain further insight into the composition and structure of the complex, we will apply the modified Fox equation (1) to lower T_g analysis. The fitting parameter w^*_{PEG}, in Eq. (1) defines a weight fraction of PEG forming two hydrogen bonds (e.g. via both terminal hydroxyls of PEG) with complementary carbonyl groups in PVP [20,21]. The w^*_{PEG}/w_{PEG} ratio outlines therefore the average molar fraction of PEG chains crosslinking the PVP units by H-bonding through both terminal hydroxyls. This quantity is plotted in Fig. 6 against PVP–PEG composition expressed as the total number of PEG OH-groups per one PVP repeat unit.

Although the DSC data in Fig. 6 refer to the PVP–PEG blends of lower hydration (6–8%), those are in excellent agreement with the TM-DSC results obtained for the blends of 12% hydration. This implies that the difference in blend hydration is properly accounted by the modified Fox equation (1), and that the effect of water on the lower T_g

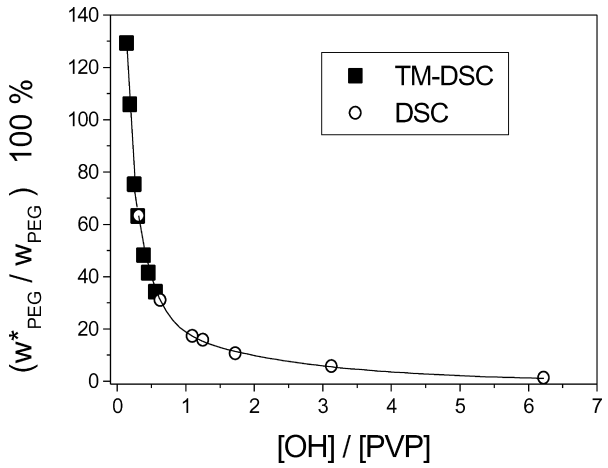

Fig. 6. The percentage of PEG-400 macromolecules crosslinking PVP units vs the number of PEG terminal OH groups available in the blends per one PVP carbonyl. Open symbols denote DSC data from Ref. [20], whereas solid symbols correspond to the values obtained using TM-DSC technique.

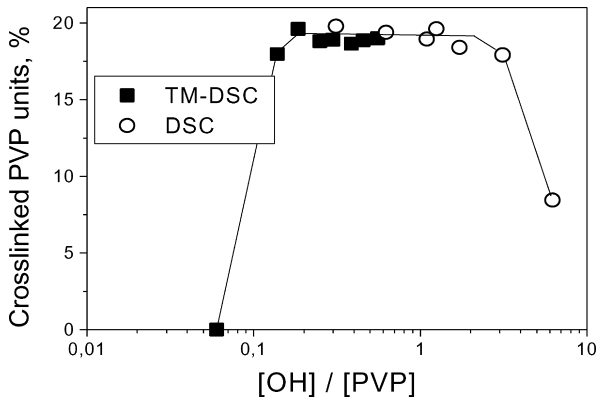

Fig. 7. Mole percent of PVP units crosslinked by PEG (via H-bonding with terminal hydroxyls) as a function of PVP–PEG blend composition expressed in terms of the number of PEG OH-groups available in the blends per one PVP repeat unit.

behaviour obeys the classical weight-average rule of mixing.

As is evident from the data in Fig. 6, at low PEG content (20 and 25%) the w^*_{PEG} fraction goes beyond w_{PEG} (the total PEG content) and the w^*_{PEG}/w_{PEG} ratio exceeds 100%. This seemingly unrealistic conclusion originates from the fact that T_g value indicates the presence of a certain phase formation within the polymer blend, but it does not define directly the amount of the formed phase. At low PEG content, the PEG chains will crosslink only some fraction of PVP macromolecules, leaving other PVP chains unoccupied. In other words, discrete nuclei of crosslinked PVP–PEG complex (lower T_g-phase) are formed within a continuous, upper T_g-phase.

3.5. Stoichiometry of the PVP–PEG complex

Taking the product of the total number of PEG OH-groups per PVP repeat unit ([OH]/[PVP]) and the molar fraction of PEG chains crosslinking the PVP units (w^*_{PEG}/w_{PEG}), we obtain the mole percent of OH groups involved into H-bonded cross-links. Assuming that every OH group forms H-bond only with a single PVP carbonyl, this product yields the mole percent of crosslinked PVP units, M^+_H [20]:

$$M^+_H = \frac{w^*_{PEG}}{w_{PEG}} \frac{[OH]}{[PVP]} 100\% \quad (3)$$

M^+_H shown in Fig. 7 is remarkably independent of PEG content within a wide composition range. This is unambiguous evidence of the PVP–PEG network complex stoichiometry. By the TM-DSC data, the amount of PVP units crosslinked through PEG chains is found to be 18.83 ± 0.24%. This is in excellent agreement with earlier reported DSC results (19.01 ± 0.54%) over a wider composition range [20,21]. We note that in our calculations, 100% accessibility of PEG hydroxyls into H-bonding has been assumed for the blends containing 20 and 25% of PEG, i.e. $w^*_{PEG} = w_{PEG}$ (see Fig. 6).

The stoichiometric composition of the PVP–PEG network complex, derived from the concentration dependence of the lower T_g, has been found to correlate fairly reasonably with the direct results of FTIR measurements as well as with the data obtained from the depression of the heat of melting of PEG in the blends with amorphous PVP [20].

3.6. Characteristics of the H-bonded network in the stoichiometric PVP–PEG complex

The existence of an H-bonding network in PVP–PEG blends has been well documented by rheological measurements [18,45]. The H-bond network ensures the rubber-like elasticity of the PVP–PEG blends. However, the characteristic features of the H-bonded network are somewhat obscured by the contribution of another network that is provided by physical junctions of long chain PVP entanglements. For this reason, the characterisation of the H-bonded network in the PVP–PEG system is of a great importance for elucidating the molecular structure of the stoichiometric complex. The analysis of the lower T_g behaviour using the modified Fox equation (1) makes this feasible. Recalling that the w^*_{PEG} quantity is defined as a weight fraction of PEG chains, which crosslink the PVP repeat units by H-bonding through both terminal hydroxyls, and taking into account that every PEG cross-link forms two H-bonds, the mole fraction of H-bonded network junctions is:

$$\frac{2w^*_{PEG}}{MW_{PEG}} \quad (4)$$

where MW_{PEG} is the PEG molecular weight (400 g/mol).

Dividing the total number of PVP repeat units in 1 g of PVP–PEG blend (w_{PVP}/MW_{PVP}) (where MW_{PVP} is the

molecular weight of the PVP monomeric unit, 111.14 g/mol) by the mole fraction of H-bond junctions (Eq. (4)) yields the average number of PVP units between neighbouring junctions:

$$\frac{w_{PVP}MW_{PEG}}{MW_{PVP}2w^{*}_{PEG}} \quad (5)$$

The critical molecular weight of PVP chain segment (M_c, g/mol) in the mesh size of H-bonded network can be estimated as:

$$M_c = \frac{w_{PVP}MW_{PEG}}{2w^{*}_{PEG}} \quad (6)$$

M_c is connected with the H-bond network density via the following equation:

$$\frac{\nu_H}{V_o} = \frac{\rho}{M_c}\ (\mathrm{mol/cm^3}) \quad (7)$$

where ρ is polymer blend density (g/cm^3), ν_H is the number of H-bonded junctions per molar volume of PVP–PEG complex, V_o. The blend density, ρ, can be evaluated as:

$$\frac{1}{\rho} = \frac{w_{PVP}}{\rho_{PVP}} + \frac{w_{PEG}}{\rho_{PEG}} + \frac{w_{H_2O}}{\rho_{H_2O}} \quad (8)$$

where $\rho_{PVP} = 1.25$, $\rho_{PEG} = 1.125$, and $\rho_{water} = 1.0$ g/cm^3, respectively.

ρ_H/V_o and M_c are shown in Fig. 8 as functions of PVP–PEG composition. Similar to the degree of crosslinking (Fig. 7), the network density (Eq. (7)) and critical molecular weight of PVP segment between neighbouring junctions of H-bonded network (Eq. (6)) remain independent of the PEG concentration within a wide composition range (20–80% of PEG-400). The average length of the PVP chain segments between the neighbouring junctions is about 5–6 PVP units, whereas the corresponding length of the PEG chain between cross-links is up to 9–10 oxyethylene units (400 g/mol). The network is fully formed at 25% of PEG content in blend, and reveals no signs of swelling or breakdown up to 80% of PEG concentration. The network formation and failure occurs in narrow ranges of composition, implying the cooperative nature of the crosslinked complex.

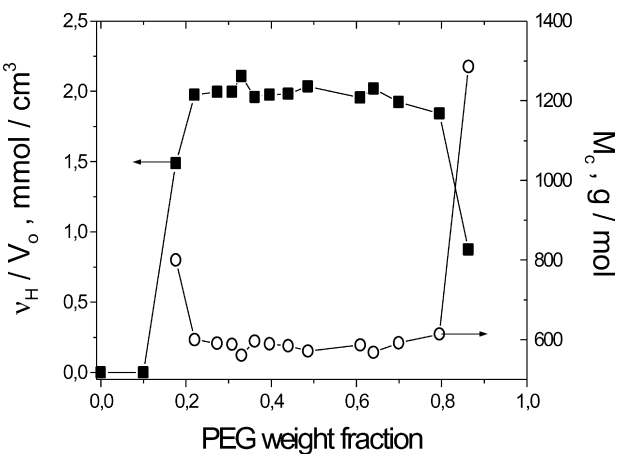

Fig. 8. Compositional dependence of the H-bonded network density, ν_H/V_o, and the critical molecular weight of PVP chain segment between neighbour PEG cross-links, M_c.

3.7. Interrelation of two glass transition temperatures and miscibility of the PVP–PEG system

As has been shown in the previous two papers of this series in the mixtures of PVP with plasticizers bearing one, two and three reactive hydroxyl groups, the negative T_g deviations from the Fox equation occur only for the plasticizers bearing more than one OH group. The larger the number of reactive groups in the plasticizer molecule, the greater the negative T_g deviations [20]. The fact that the upper T_g of the PVP–PEG blend obeys fairly reasonably the classical form of the Fox equation ($w^{*}_{PEG} = 0$, Fig. 3) implies that the upper T_g-phase corresponds to a homogeneous PVP–PEG mixture, or PVP solution in PEG, where in average each PEG molecule forms only a single H-bond with the PVP carbonyl, leaving the second OH group, at the opposite chain end, free.

As discussed above, the lower T_g-phase is found to be related to the PVP–PEG complex formation, where the PVP units are crosslinked by H-bonding through both terminal groups of PEG short chains. In the PVP–PEG blends, the complex behaves like a new entity with distinctive physical properties. Taking into consideration the network structure of the complex that is formed within the upper T_g-phase representing the PVP solution in PEG, the lower and the upper T_g phases may be, respectively, defined as 'gel' and 'sol' phases. As is seen from Fig. 7, the fraction of crosslinked PVP units considerably increases with an increase of PEG content. It is logical to propose that the lower T_g, gel phase (stoichiometric crosslinked complex) is formed within the upper T_g, sol phase (constituted by a homogeneous PVP solution in PEG). The lower T_g component is not spatially separated from the upper T_g component, representing a homogeneous mixture on a molecular scale and a single common phase. The full transparency of PVP–PEG blends in UV-light indicates the absence of phase separation on a dimension scale of 100–200 nm and larger as confirmed by the WMI techniques. No evidence of the phase separation or phase boundaries has been observed in the course of microinterferometric examination of spontaneous PVP mixing with PEG, indicating unlimited glassy polymer dissolution in liquid PEG-400 [17,22]. However, the possibility of local self-organisation on a submicroscopic level should not be totally ruled out. There has been a considerable discussion in the literature as to the level of dispersion necessary for the observation of a single T_g, with the segmental motions associated with the glass transition encompassing a domain size on the order of 2–15 nm [54,55]. This means that the occurrence of two T_gs in the PVP–PEG blends may be the result of phase separation on a nanoscale, within size range

of 2–200 nm. Therefore, complementary methods such as neutron scattering have to confirm the molecular arrangements of PVP–PEG mixing.

As is noted above, the additional criterion for miscibility on a molecular scale allowing the distinction of the miscible blends from those very close to being miscible is the consistency of behaviour of all thermal transitions occurring in truly miscible blends [25–27]. Consequently, in order to define whether the PVP–PEG system is miscible within the concentration region where two glass transitions occur (in the range between 20 and 50% of PEG), we have to check the consistency of the upper and lower T_gs. If two transitions are consistent, the system can be considered as miscible in the whole concentration range, because beyond the two T_g region the PVP–PEG system has been already found to be truly miscible [18,20,21,25–27,30].

As follows from the data in Fig. 3, while the original form of the Fox equation is mainly valid to describe adequately the compositional profile of the upper T_g, comparatively small negative T_g deviations still occur. These deviations cannot be fitted adequately by assuming that in reality the blend hydration is somewhat higher than the measured value of 12%. To be certain in this fact, let us consider the weight fraction of water in PVP–PEG blend as an adjusting parameter in the Fox equation and find a hypothetical hydration using Eq. (9):

$$\frac{1}{T_g} = \frac{w_{PVP}(1 - w_{H_2O})}{T_{g_{PVP}}} + \frac{w_{PEG}(1 - w_{H_2O})}{T_{g_{PEG}}} + \frac{w_{H_2O}}{T_{g_{H_2O}}} \quad (9)$$

As calculations have shown, the obtained upper T_g values in principle can be fitted reasonably well, however only if the hydration is allowed to be as high as 15.4, 16.3, 18.3 and 22.7% for the blends containing 20, 31, 35 and 41% of PEG-400, respectively. As one can see, to match the experimental data one has to assume changing (increasing) water fraction as the PEG content increases that does not correspond to experimental reality.

It is worthwhile to note that the negative upper T_g deviations take place only in the concentration range where two glass transitions are observed (Fig. 3). This implies that two T_gs are somewhat interrelated and evolve in a systematic (self-consistent) way with blend composition. Let us assume that the stoichiometric PVP–PEG complex (network) with the lower T_g is immiscible on a molecular scale with the homogeneous PVP–PEG mixture characterised by the upper T_g. If so, a fraction of PVP units and PEG chains involved into the stoichiometric crosslinked complex is inaccessible for homogeneous mixing with PEG in the upper T_g-phase and may be responsible for the negative upper T_g deviations. In this case, the upper T_g behaviour is thought to obey the Fox equation in its following modified form:

$$\frac{1 - w^*_{PVP} - w^*_{PEG}}{T_g} = \frac{w_{PVP} - w^*_{PVP}}{T_{g_{PVP}}} + \frac{w_{PEG} - w^*_{PEG}}{T_{g_{PEG}}} + \frac{w_{H_2O}}{T_{g_{H_2O}}} \quad (10)$$

where the w^*_{PVP} is the weight fraction of crosslinked PVP units and w^*_{PEG}, as before, is the weight fraction of PEG chains crosslinking the PVP units. Since every PEG chain is capable of crosslinking simultaneously two PVP units, the w^*_{PVP} and w^*_{PEG} quantities are interrelated by the expression:

$$w^*_{PEG} = \frac{w^*_{PVP}}{2}\frac{MW_{PEG}}{MW_{PVP}} = 1.7795 w^*_{PVP} \quad (11)$$

Eq. (10) implies that PEG chains, crosslinking PVP units, are partially accumulated within the lower T_g-phase (corresponding to the stoichiometric PVP–PEG complex), and therefore unable to plasticize in sufficient extent the glassy PVP in the upper T_g, sol phase. However, these attempts to fit the experimental upper T_g points in Fig. 3 with Eq. (10) failed, yielding irrelevant (negative) w^*_{PVP}. The failure of Eq. (10) to describe the upper T_g behaviour may imply that the PEG chains crosslinking PVP units via H-bonds through their terminal hydroxyls, are not immobilised completely in the stoichiometric PVP–PEG complex, but capable of exchanging with other PEG chains, which are bound with PVP only by single H-bond. Indeed, the act of such an exchange is simply a rupture of one H-bond, while the other OH group at the opposite PEG chain end remains H-bonded. In contrast to the non-cooperative behaviour of PEG chains, the PVP units are interconnected into long polymer chains, and the state of every repeat unit is influenced by the state of its neighbours. Some fraction of PVP chains may prefer to remain unconnected to the hydrogen bonded PVP–PEG network, as it would lead to a considerable loss of translational entropy. These PVP chains constitute the upper T_g phase. Hence, the process of H-bonding of PVP units to PEG terminal hydroxyls may be expected to have a cooperative character with PEG chains being shared between crosslinked and free PVP chains, i.e. between lower and upper T_g phases. In this case, the crosslinked PVP units are eliminated from the interaction with PEG and the compositional behaviour of the upper T_g should follow the equation:

$$\frac{1 - w^*_{PVP}}{T_g} = \frac{w_{PVP} - w^*_{PVP}}{T_{g_{PVP}}} + \frac{w_{PEG}}{T_{g_{PEG}}} + \frac{w_{H_2O}}{T_{g_{H_2O}}} \quad (12)$$

Using Eq. (12), the fitting w^*_{PVP} parameter was evaluated from the compositional profile of the upper T_g. The percent of PVP units inaccessible for plasticization with PEG in the upper T_g-phase due to their crosslinking and segregation into stoichiometric PVP–PEG complex in gel phase was calculated as $(w^*_{PVP}/w_{PVP})100\%$. The percent of PVP units unavailable for plasticization in the upper T_g, sol phase was

Table 1
The w^*_{PVP} parameter calculated using Eq. (13) and the percent of PVP units inaccessible for plasticization with PEG in the upper T_g-phase $(w^*_{PVP}/w_{PVP})100\%$

w_{PEG}	w_{PVP}	w_{water}	w^*_{PVP}	$(w^*_{PVP}/w_{PVP})100\%$
0.176	0.704	0.12	0.1253	17.23
0.273	0.607	0.12	0.1138	18.74
0.308	0.572	0.12	0.1476	25.70
0.361	0.379	0.12	0.0831	16.01

found to be 19.42 ± 0.02% (Table 1). The obtained value is in excellent agreement with the percent of PVP units crosslinked by H-bonding through PEG chains, $M_H^+ = 18.83 \pm 0.24\%$ (see Eq. (3)), which was found earlier from the analysis of the lower T_g behaviour using Eq. (1) and is shown in Fig. 7.

The implication of the established correlation is that the upper and the lower T_gs are influenced by each other (i.e. consistent), signifying that the PVP–PEG system is truly miscible despite the occurrence of two distinct glass transitions. The cooperative mechanism of PVP–PEG complex formation is typical of sorption of low molecular weight ligands with high molecular weight polymers. In this process, the short chain PEG behaves like the low molecular weight ligand.

3.8. The phase behaviour of the PVP–PEG system throughout the entire composition range

Fig. 9 and Table 2 summarise our view on the mechanism of glassy PVP dissolution in liquid PEG outlined by the data presented in Figs. 3–8. At low PEG concentrations (0–20%), the PVP plasticization occurs, leading to the decrease of the T_g of the blend that follows fairly reasonably the Fox rule of mixing (Fig. 3). Such mixing is typical for miscible systems and is characteristic of the formation of a single-phase, homogeneous solution. However, as the PEG content reaches 20%, the gel of PVP crosslinked by H-bonding with PEG chains begins to appear, evidenced by the occurrence of the second glass transition. In principle, the smaller the PEG content, the higher the involvement of PEG hydroxyl groups into PVP crosslinking (Fig. 6). Then, it is not clear why the PVP–PEG crosslinked complex is formed only at 20% PEG concentration. In part, the answer lies in the fact that the PVP–PEG crosslinked complex requires a specified amount of PEG for its formation. Indeed, the data in Figs. 3, 5, 7–9 and Table 2 show, that the stoichiometric complex involves 18–19% of PVP units crosslinked by PEG terminal hydroxyls (via H-bonding) that requires about 14 OH-groups of PEG per 100 PVP units (26 wt% of PEG-400 in blends).

As is seen from Figs. 3 and 9, the upper T_g has to be in the vicinity of 20 °C in order for the lower T_g-phase to appear. Let us recall that these blends are plasticized additionally with 12% of sorbed water. In dry blends to achieve the same upper T_g value the PEG concentration should be as large as 40% (Figs. 3 and 5), compared to 26 wt% for the wet blends considered here. It remains to be explored whether the stoichiometric complex can be formed in dry blends containing 26% of PEG, since in this case the upper T_g is as high as 70 °C, and the elevation in temperature is known to result in the weakening of H-bonds.

Actually, to achieve the necessary level of crosslinking by hydrogen bonding, not only the PEG content should be large enough, but also the temperature should be sufficiently low. Both of these factors enhance hydrogen bond formation. To achieve the same average degree of hydrogen bonding between PVP and PEG at higher temperature the larger amount of PEG would required.

Thus, the upper T_g value is a critical factor controlling the onset of the stoichiometric complex formation. Apart from the effect of blend hydration, the upper T_g depends also

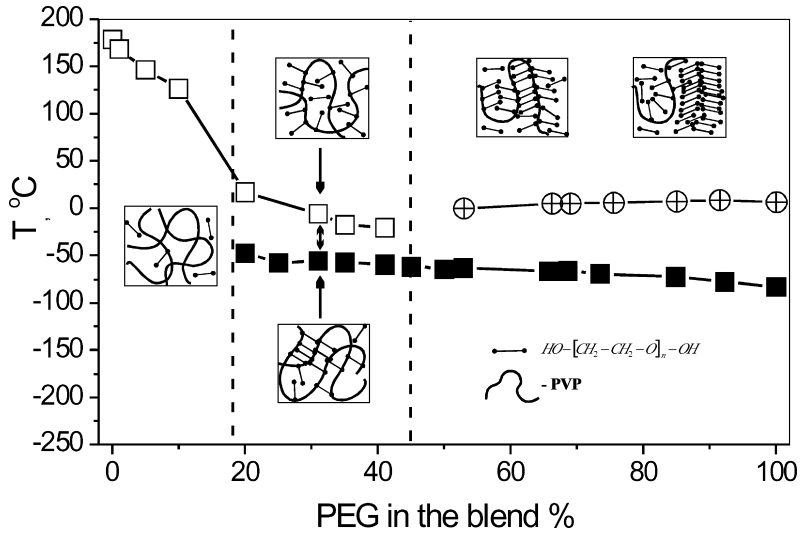

Fig. 9. Schematic presentation of the scenario of PVP dissolution in liquid PEG along with the data from Fig. 2 (open and solid squares) and meting transition temperature for PEG (circles with cross).

Table 2
Phase state of the PVP–PEG system and underlying molecular mechanisms corresponding to different stages of the dissolution of glassy PVP in liquid PEG

% PEG	$[OH]_{PEG}/[PVP]$	Stage of spontaneous PVP–PEG mixing	Composition	Phase state
0–10	0–0.06	(1) Homogeneous PVP–PEG mixing	Homogeneous PVP–PEG mixture	Single amorphous phase with T_g obeying the Fox rule of mixing for dry blends + water in vapour state
10–20	0.06–0.14		Homogeneous PVP–PEG–water mixture	Single amorphous phase with T_g obeying the Fox rule of mixing for hydrated blends
20–35	0.14–0.3	(2) Stoichiometric PVP–PEG H-bond complex formation within homogeneous PVP–PEG mixture	Homogeneous PVP–PEG mixture + stoichiometric complex	Two amorphous phases with different composition-dependent T_gs
35–41	0.3–0.39		Stoichiometric PVP–PEG complex + homogeneous PVP–PEG mixture	Two amorphous phases with different composition-dependent T_gs; presumably phase inversion
45–80	0.46–2.22	(3) Dissolution of PVP–PEG stoichiometric complex in excess PEG	Mixing the stoichiometric PVP–PEG complex with excess PEG: PVP–PEG complex + PEG	Single amorphous phase (above PEG T_m); Amorphous–crystalline phase separation (below PEG T_m)
80–90	2.22–5.0		H-bonded network failure and gradual disengagement of PVP chains from the stoichiometric complex: PVP–PEG complex + PVP–PEG mixture	
>90	>5.0		PVP solution in PEG	

on PVP molecular weight, decreasing appreciably with the decrease in polymer chain length.

It is well known from the literature that polymer crosslinking causes usually an increase in T_g [56,57]. Nevertheless, in PVP–PEG systems the PVP crosslinking through PEG chains results in appreciable T_g reduction compared with uncrosslinked PVP in the upper T_g-phase at equivalent PEG concentrations (Figs. 3 and 9). Apparent anomalous behaviour of the PVP–PEG blends has also been shown to be due to the appreciable length and the flexibility of PEG chains, which couple the properties of H-bonding crosslinker and spacer [18,21,25–27]. Creating a space between longer PVP macromolecules, the PEG chains increase the free volume and, eventually, the molecular mobility of PVP chain segments between neighbour H-bond network junctions [37,38]. Crosslinking PVP units by H-bonding to PEG terminal hydroxyls, the PEG chains behave also as a cohesive toughness enhancer [47]. It is because of combining the properties of both cohesive strength and free volume enhancer, that the short chain PEG is believed to be responsible for pressure-sensitive adhesion. This self-adhesive behaviour has been earlier reported to appear in a very narrow range of the PVP–PEG compositions and to be affected by the degree of blend hydration [45–52].

As follows from the data in Fig. 6, with the rise in PEG concentration, the involvement of its chains in the crosslinking of PVP is reduced. The relative amount of the lower T_g-phase increases gradually, and as the PEG content achieves 35%, a phase inversion is thought to occur when the lower T_g-phase becomes dominant. The composition where this phase inversion takes place is believed to be outlined by an abrupt growth of the relevant ΔC_p value in Fig. 4. This hypothesis needs further experimental confirmation.

As the content of crosslinked monomer units in all PVP chains achieved its stoichiometric value (19%), the upper T_g vanishes. This occurs within the range of PEG concentrations between 41 and 50% (Figs. 3, 5 and 9). Subsequent mixing of the complex with excess PEG is accompanied by the appearance of a crystalline PEG phase below its melting temperature, T_m (Figs. 5 and 9 and Table 2). Within relatively diluted PVP solutions, containing 80–90% of solvent (PEG-400), the swelling of the PVP–PEG H-bonded network is thought to occur (Figs. 7 and 8). The concentration region where the PEG content is more than 90% corresponds already to PVP solutions in PEG-400.

3.9. Equilibrium constant of the PVP–PEG complex formation

Figs. 7 and 8 provide an insight into the structure and composition of the lower T_g-phase only and demonstrate a remarkable stoichiometry of the crosslinked PVP–PEG H-bonded complex. With the increase in PEG concentration above 40% (Figs. 5 and 9, Tables 1 and 2), the content of the complex in the blend decreases, maintaining constant the fraction of crosslinked PVP units. Actually, the amount of crosslinked PVP units relates directly to w^*_{PEG} quantity, whereas according to Eq. (3) the fraction of crosslinked PVP units is defined by the w^*_{PEG}/w_{PEG} factor. The negative T_g deviations and, correspondingly, the w^*_{PEG} parameter decline gradually with the PEG concentration above 40% (Figs. 3 and 5), while the latter is kept constant until nearly 80% PEG (Figs. 7 and 8).

The process of PVP–PEG complex formation may be treated as a chemical equilibrium, described by the constant K_H^+ (mol/g), which can be expressed in terms of the w^*_{PEG} and w_{PEG} as follows [21]:

$$K_H^+ = \frac{2w^*_{PEG}}{(2w_{PEG} - w^*_{PEG})\left(\frac{w_{PVP}}{MW_{PVP}} - \frac{2w^*_{PEG}}{MW_{PEG}}\right)} \quad (13)$$

An addition or removal of one of the reactants or the product shifts the position of the sol–gel equilibrium accordingly. Consequently, K_H^+ varies with blend composition as shown in Fig. 10. K_H^+ is a measure of the tendency of the complexation to occur. If it is a large and positive number (and the concentration of reactants is not too small), the concentration of PVP–PEG complex is large compared to those of still available reactants, [OH] and [PVP]. This is the case for the blends containing excess PVP, i.e. the stage of a strong PVP–PEG interaction and stoichiometric complex formation ($w_{PEG} = 0.2–0.45$). At the stage of H-bonded network failure (due to gel swelling in excess of PEG) followed by the PVP dissolution ($w_{PEG} > 0.8$), the K_H^+ constant drops significantly, tending to zero at large PEG overloading. Within the intermediate concentration region (at the stage of complex mixing with PEG), the curve in Fig. 10 demonstrates a comparatively stable K_H^+ behaviour. In this manner, the boundaries between the three different stages of the process of PVP spontaneous dissolution in liquid PEG correlate very well with those indicated in Fig. 9 and Table 2. Again, the TM-DSC data are in a good agreement with earlier reported DSC results [21].

Since PVP is soluble in PEG, the PVP–PEG blends can be treated as PVP solutions in PEG. Accordingly, the equilibrium between the lower T_g-phase (PVP–PEG crosslinked H-bond complex) and the upper T_g-phase (PVP solution in PEG) can be considered as the complex dissociation equilibrium. Using the approach described in two preceding papers of this series and based on the modified Fox equation (1) [20,21], the equilibrium between crosslinked PVP units (in the lower T_g-phase) and those free of crosslinking (in the upper T_g-phase) may be evaluated in terms of dissociation degree (α) :

$$\frac{\alpha^2}{1-\alpha} = \frac{MW_{PEG}}{K_H^+ 2w^*_{PEG}} \quad (14)$$

The term ($2w^*_{PEG}/MW_{PEG}$) is the mole fraction of PEG OH-groups involved into H-bonding and crosslinking the PVP units per 1 g of the blend, which is equal to the mole fraction of crosslinked PVP units.

The dissociation degree monotonously increases with PEG content (Fig. 10). With the rise in PEG concentration α tends towards 1, indicating complete dissociation of network complex. In contrast, within concentrated PVP solutions (at the stage of complex formation, Fig. 9, Table 2) the dissociation degree achieves 0.81, implying that 19% of PVP units are only crosslinked in the stoichiometric complex.

The equilibrium constant of the PVP–PEG stoichiometric complex formation provides a bridge to the standard free energy change for PVP–PEG association into a hydrogen-bonded crosslinked stoichiometric complex, ΔG_H^+. The latter relates to the equilibrium constant through the fundamental van't Hoff equation:

$$\Delta G_H^+ = -RT \ln K_H^+ \quad (15)$$

The composition dependence of the free energy for PVP curing by hydrogen bonding through PEG short chains is presented in Fig. 11. Large K_H^+ values correspond to the large negative ΔG_H^+ magnitudes. The PVP–PEG complex formation is an exothermic process. The gain in energy is greater at the first stage of PVP plasticization due to hydrogen bonding with PEG ($w_{PEG} = 0.2–0.45$), than at the subsequent stages of mixing of the PVP–PEG complex with PEG followed by the swelling of H-bonded network and dissolution of disengaged PVP macromolecules in excess PEG (Figs. 7–9).

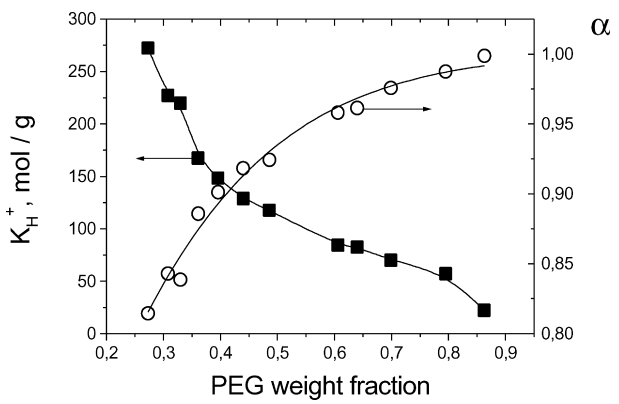

Fig. 10. The composition dependence of the constant of PVP–PEG stoichiometric complex formation, K_H^+ (mol/g) and the degree of dissociation, α.

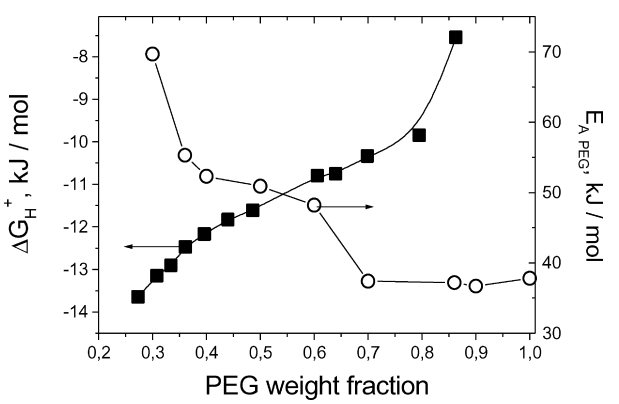

Fig. 11. Free energy change (ΔG_H^+, kJ/mol) for the stoichiometric PVP–PEG complex formation and the activation energy for PEG self-diffusion, E_A [37], as a function of PVP–PEG composition.

3.10. Comparison of the T_g analysis data with the results of independent measurements

DSC scans characterise the heat capacity as a function of temperature. In turn, the heat capacity is a measure of molecular mobility that relates to the energy of cohesive interaction and free volume. Traditionally, the molecular mobility of macromolecules is evaluated in terms of self-diffusion coefficients. They have been measured for the PVP–PEG systems by a PFG NMR technique in relation to the composition, hydration, molecular weights of components involved and temperature [37,38]. The composition profiles of the activation energy for PEG-400 self-diffusion in the blends with high molecular weight PVP (E_A) and the energy of crosslinking PVP units (ΔG_H^+) are compared in Fig. 11. At the stage of crosslinked complex formation ($w_{PEG} < 0.4$), the PVP–PEG interaction is especially strong, and the E_A curve reveals an abrupt increase (with a decrease in PEG content) implying that PEG loses its diffusivity due to its involvement into the crosslinked PVP–PEG complex. When the complex is mixed with unbound PEG that is capable of crystallising below T_m ($w_{PEG} = 0.4–0.8$, Figs. 5 and 9 and Table 2), the equilibrium constant of PVP crosslinking reduces (Fig. 10) and the PVP–PEG interaction becomes weaker (Fig. 11). Correspondingly, the E_A decreases at this stage. At last, as the PEG concentration achieves 70–80%, the failure of the PVP–PEG network complex occurs (Figs. 7 and 8) due to the corresponding decrease of crosslinking energy (Fig. 11). Within this concentration range, the complex dissociates (Fig. 10), and the activation energy for PEG self-diffusion matches closely the value found for bulk PEG-400 ($E_A = 38$ kJ/mol, Fig. 11). This indicates that PEG interaction with PVP provides no obstacles for PEG diffusion in diluted polymer solutions containing more than 70% of the solvent (PEG-400). Thus, the composition profile of diffusivity of short-chain PEG in the blends with PVP (evaluated with the PFG NMR method) follows the pattern of the free energy of PVP H-bond crosslinking, obtained from the analysis of the deviations of the lower T_g from weight-average values using the modified Fox equation (1).

It has also been shown by wedge interferometry that diffusion of short chain PEG in the blends overloaded with low molecular weight PVP is restricted by a kind of entanglement process which resembles chain reptation [22]. Since the chain reptation is thought to be a rather untypical mode of diffusion for such highly flexible and short macromolecules as oligomeric PEG-400, the observed effect has been explained by the process of PEG chain engagement into H-bonded network formed in the PVP–PEG blends.

Both heat capacity and diffusivity are microscopic properties of PVP–PEG blends. The macroscopic properties, such as rubber-like viscoelasticity and pressure sensitive character of adhesion, involve numerous processes acting on a molecular level. It comes therefore as no surprise that evident correlation has been established between the mechanism of PVP–PEG interaction discussed above and the composition dependence of viscoelastic and adhesive properties of the PVP–PEG blends [45–51]. In particular, the composition profile of the activation energy for adhesive debonding of the PVP–PEG hydrogels has been found to follow the pattern known for the activation energy for PEG self-diffusion, implying the importance of the contribution of the molecular mobility to adhesive polymer behaviour [51]. Other correlations between the stoichiometric composition of the PVP–PEG complex obtained with FTIR spectroscopy and that derived from the T_g analysis using the w^*_{PEG} parameter are reviewed in the second paper of this series [21].

4. Conclusions

The PVP–PEG system is plausibly among the first and most illustrative examples of miscible single-phase polymer blends, which reveal two distinct glass transition temperatures with coherent compositional behaviour. The behaviour of the upper T_g in PVP–PEG blends has been found to obey the well-known Fox equation, indicating homogeneous PVP–PEG mixing, or glassy PVP dissolution in liquid PEG. At the same time, the lower T_g is due to the formation of hydrogen bonded PVP–PEG network complex (gel), which behaves like a new chemical entity. In the stoichiometric complex, nearly 20% of PVP repeat units have been shown to be crosslinked by PEG terminal OH-groups (via H-bonding). Due to the considerable length and flexibility of the PEG chains they create a space between longer PVP macromolecules, coupling enhanced energy of cohesive interaction with a large free volume. These factors are responsible for the lower T_g value found for the phase of crosslinked PVP–PEG complex as compared with the upper T_g featured for the uncrosslinked PVP–PEG mixture.

The upper and lower T_g-phases display disparate physical properties (e.g. heat capacity). In the uncrosslinked complex related to the upper T_g-phase, PEG chains interact with PVP through one terminal group only. This labile complex requires a comparatively small amount of heat for dissociation. In contrast, the lifetime of crosslinked PVP–PEG complex is much longer (as shown using PFG NMR) due to multiple hydrogen bonds involved in its formation.

Analyses of upper T_g behaviour provides an evidence of the cooperative mechanism of PVP–PEG stoichiometric complex formation. The cooperative behaviour is mainly featured for the high molecular weight polymer, PVP, while the short-chain PEG behaves like a low molecular weight ligand and demonstrates a rather homogeneous distribution among the upper and lower T_g-phases. Besides, in the composition range characterised by two T_gs there have been no signs of crystallization observed ruling out the possibility of macrophase separation. This is also have been confirmed

by WMI technique. Thus, we conclude that the lower T_g phase is formed inside the upper T_g phase. Both phases share PEG chains, but have different level of involvement of PEG chains in hydrogen bonding (cross-linking) leading to observed two T_g behaviour.

The process of spontaneous dissolution of glassy PVP in liquid PEG-400 consists of three successive stages occurring in different composition regions. At low PEG concentration, the formation of single hydrogen bonds between PEG end-groups and PVP units leads to a decrease of T_g of the homogeneous mixture. The decrease of the T_g becomes more pronounced at higher PEG content. Within PVP-rich blends with 20–40% of PEG, the involvement of PEG terminal hydroxyls into H-bonding with PVP carbonyls reaches nearly 100%. Since H-bonding of PEG chains through both terminal OH-groups results in the crosslinking of the PVP units, this stage is defined as the PVP–PEG network complex formation and characterised by two T_gs. One of them corresponds to the PVP–PEG complex (gel phase) and another one to the homogeneous PVP/PEG mixture (sol phase). The PVP–PEG interaction at this stage is especially strong. With further increase in PEG concentration, the stage of complex formation is altered by the mixing of the PVP–PEG crosslinked complex with excess PEG (solvent). An appearance of PEG unengaged in H-bonded network formation results at this stage in the rise of blend crystallinity below the fusion temperature of PEG and in the disappearance of the upper T_g. The composition of the PVP–PEG network complex exhibits a remarkable stoichiometry throughout the stages of the complex formation and mixing with excess PEG. Finally, at high PEG content the failure of the PVP–PEG network occurs. Both the complex formation and dissociation have cooperative character, and take place in a narrow composition range.

Acknowledgements

The research of the Russian scientist was in part made possible by Award No. RC1-2057 of the US Civilian Research & Development Foundation (CRDF). E.E.D. thanks University of Minnesota MRSEC Program (Award DMR-9809364) for financial support. We express our appreciation to Prof. Nicolai A. Platé for helpful discussion and comments.

References

[1] Paul DR, Newman S. Polymer blends. New York: Academic Press; 1978.
[2] Paul DR, Bucknall CB. Polymer blends. New York: Wiley; 2000.
[3] Painter PC, Coleman MM. In: Paul DR, Bucknall CB, editors. Polymer blends, vol. 1. New York: Wiley; 2000. p. 93–140.
[4] Coleman MM, Graf JF, Painter PC. Specific interactions and the miscibility of polymer blends. Lancaster, PA: Technomic Publishing Inc; 1991.
[5] Coleman MM, Narvet LA, Painter PC. Polymer 1998;39(23):5867–9.
[6] Lee NY, Painter PC, Coleman MM. Macromolecules 1988;21(4): 954–9.
[7] Moore JA, Kaur S. Macromolecules 1998;31:328–35.
[8] Chan Ch-K, Chu I-M. Polymer 2001;42:6089–93.
[9] Prinos J, Panayiotou C. Polymer 1995;30(6):1223–7.
[10] Slark AT. Polymer 1997;38(10):2407–14.
[11] Meensen F, Nies E, Berghmans H, Verbrugghe S, Goethals E, Du Prez F. Polymer 2000;41:8597–602.
[12] Kirsh YE. Water soluble poly(*N*-vinylamides). New York: Wiley; 1998.
[13] Sakellariou P, Abraham MH, Whiting GS. Colloid Polym Sci 1994; 272(7):872–5.
[14] Cesteros LC, Quintana JR, Fernandez JA, Katime IA. J Polym Sci, Polym Phys Ed 1989;27:2567–76.
[15] Spitzer M, Sabadini E, Loh W. J Braz Chem Soc 2002;13:7–9.
[16] Buehler V. Kollidon: polyvinylpyrrolidone for the pharmaceutical industry, 3rd ed. Ludwigshafen: BASF; 1996. pp. 19–20.
[17] Bairamov DF, Chalykh AE, Feldstein MM, Siegel RA, Platé NA. J Appl Polym Sci 2002;85:1128–36.
[18] Feldstein MM, Lebedeva TL, Shandryuk GA, Kotomin SV, Kuptsov SA, Igonin VE, Grokhovskaya TE, Kulichikhin VG. Polym Sci 1999; 41(8):854–66.
[19] Feldstein MM, Lebedeva TL, Shandryuk GA, Igonin VE, Avdeev NN, Kulichikhin VG. Polym Sci 1999;41(8):867–75.
[20] Feldstein MM, Shandryuk GA, Platé NA. Polymer 2001;42(3):971–9.
[21] Feldstein MM, Kuptsov SA, Shandryuk GA, Platé NA. Polymer 2001; 42(3):981–90.
[22] Bairamov DF, Chalykh AE, Feldstein MM, Siegel RA. Macromol Chem Phys 2003; in press.
[23] Fox TG. Bull Am Phys Soc 1956;1:123.
[24] MacKnight WJ, Karasz FE, Fried JR. In: Paul DR, Newman S, editors. Polymer blends. New York: Academic Press; 1978. Chapter 5.
[25] Feldstein MM, Shandryuk GA, Kuptsov SA, Platé NA. Polymer 2000; 41(14):5327–38.
[26] Feldstein MM, Kuptsov SA, Shandryuk GA. Polymer 2000;41(14): 5339–48.
[27] Feldstein MM, Kuptsov SA, Shandryuk GA, Platé NA, Chalykh AE. Polymer 2000;41(14):5349–59.
[28] Askadskii AA, Matveev YuI. Chemical structure and physical properties of polymers. Chemistry (Moscow) 1983;24–48.
[29] Tager AA. Physicochemistry of polymers, 3rd ed. Moscow: MIR; 1978. Chapter 16.
[30] Feldstein MM. Polymer 2001;42(18):7719–26.
[31] Gordon M, Taylor JS. J Appl Chem 1952;2:493–500.
[32] Couchman PR, Karasz PE. Macromolecules 1978;11(1):117–9.
[33] Braun G, Kovacs AJ. In: Prins JA, editor. Physics of non-crystalline solids. Amsterdam: North-Holland; 1965.
[34] Kwei TK. J Polym Sci, Polym Lett 1984;22(6):307–13.
[35] Breckner MJ, Schneider HA, Cantow HJ. Makromol Chem 1988;189: 2085–97.
[36] Di Marzio EA. Polymer 1990;31(12):2294–8.
[37] Vartapetian RSh, Khozina EV, Kärger J, Geschke D, Rittig F, Feldstein MM, Chalykh AE. Macromol Chem Phys 2001;202(12): 2648–52.
[38] Vartapetian RS, Khozina EV, Kärger J, Geschke D, Rittig F, Feldstein MM, Chalykh AE. Colloid Polym Sci 2001;279(6):532–8.
[39] Reading M. Trends Polym Sci 1993;8(1):248–53.
[40] Gill PS, Sauerbrunn SR, Reading M. J Thermal Anal 1993;40:931–9.
[41] Reading M, Elliot D, Hill VL. J Thermal Anal 1993;40:949–55.
[42] Reading M, Luget A, Wilson R. Thermochim Acta 1994;238: 295–307.
[43] Sauer BB, Kampert WG, Neal Blanchard E, Threefour SA, Hsiao BS. Polymer 2000;41:1099–108.

[44] Kotomin SV, Borodulina TA, Feldstein MM, Kulichikhin VG. Proc XIII Int Cong Rheol, Cambridge, UK 2000;4:44–6.
[45] Roos A, Creton C, Novikov MB, Feldstein MM. J Polym Sci, Polym Phys 2002;40:2395–409.
[46] Chalykh AA, Chalykh AE, Novikov MB, Feldstein MM. J Adhesion 2002;78(8):667–94.
[47] Feldstein MM, Platé NA, Chalykh AE, Cleary GW. Proc 25th Annu Meeting Adhesion Soc 2002;292–4.
[48] Feldstein MM, Chalykh AE, Chalykh AA, Platé NA. Polym Mater Sci Engng 1999;81:465–6.
[49] Feldstein MM, Chalykh AE, Chalykh AA, Fleischer G, Siegel RA. Polym Mater Sci Engng 1999;81:467–8.
[50] Feldstein MM, Chalykh AE, Platé NA. Proc Fifth Eur Conf Adhesion (EURADH'2000), Lyon, France 2000;176–81.
[51] Feldstein MM, Borodulina TA, Vartapetian RSh, Kotomin SV, Kulichikhin VG, Geschke D, Chalykh AE. Proc 24th Annu Meeting Adhesion Soc 2001;137–40.
[52] Roos A, Creton C, Feldstein MM. Proc 24th Annu Meeting Adhesion Soc 2001;277–9.
[53] Tanaka N. Polymer 1978;19(7):770–2.
[54] Utracki LA. Polymer alloys and blends: thermodynamics and rheology. New York: Hanser; 1990.
[55] Kalika DS. In: Paul DR, Bucknall CB, editors. Polymer blends, vol. 1. New York: Wiley; 2000. p. 291–317.
[56] Bershtein VA, Egorov VM. Differential scanning calorimetry of polymers. New York: Horwood; 1994.
[57] Maes C, Devaux J, Legras R, McGrail PT. Polymer 1995;36(16): 3159–64.